

Articles

Structure and Nonlinear Optical Properties of the Cubic Cage Complex $(n\text{-Bu}_4\text{N})_3[\text{Cu}_3\text{MoOS}_3\text{BrI}_3]$

Patrick E. Hoggard^{*,†}

Department of Chemistry, North Dakota State University, Fargo, North Dakota 58105

Hong-Wei Hou, Xin-Quan Xin, and Shu Shi^{*}

Department of Chemistry, Nanjing University, Nanjing, Jiangsu, China 210008

Received August 2, 1995. Revised Manuscript Received June 4, 1996[⊗]

Unlike the analogous $(n\text{-Bu}_4\text{N})_3[\text{Cu}_3\text{MoOS}_3\text{Br}_4]$, in which the cluster has a partially open cage structure, in the salt $(n\text{-Bu}_4\text{N})_3[\text{Cu}_3\text{MoOS}_3\text{BrI}_3]$ the anion forms a cubane-like cluster, consisting of a (Cu_3Mo) tetrahedron interlocked with an (S_3I) tetrahedron. The solid crystallizes in the cubic space group $F\bar{4}3c$ ($a = 24.422(3)$ Å; $Z = 8$), the cluster adopting 12 allowed orientations randomly. This material exhibits a strong nonlinear optical absorption and a large, self-defocusing refractive index change. This behavior is intermediate between that of analogous nest-shaped clusters with an $\text{Mo}=\text{O}$ group and cubic cage clusters with an $\text{Mo}=\text{S}$ group, indicating that both the nature of the metal–chalcogenide and the overall skeletal structure of the cluster influence the nonlinear optical properties of the material.

Introduction

A previous study drew attention to the nonlinear optical (NLO) properties of M_4N_8 clusters ($\text{M} = \text{metal}$, $\text{N} = \text{nonmetal}$).¹ Perhaps the most significant of these was optical limiting, the increase in extinction coefficient at high light intensity. The structures of related inorganic clusters appear to have a considerable influence on the NLO properties.^{2–6} It has been observed that cubic cage-shaped clusters $[\text{MM}'_3\text{BrX}_3\text{S}_4]^{3-}$ exhibit a large NLO absorption but only a very small, self-defocusing NLO refraction, whereas nest-shaped clusters exhibit a moderate NLO absorption but a very large, self-defocusing NLO refraction.⁴

Several examples are known of cubane-like clusters that belong to cubic space groups because of a statistical distribution of atoms. These include $(\text{Bu}_4\text{N})_3[\text{MoAg}_3\text{S}_4\text{BrI}_3]$,⁷ $(\text{Bu}_4\text{N})_3[\text{MoAg}_3\text{S}_3\text{OBr}_4]$,⁸ $(\text{Bu}_4\text{N})_3[\text{WAg}_3\text{S}_4\text{Cl}_4]$,⁹ and $(\text{Et}_4\text{N})_3[\text{WCu}_3\text{S}_4\text{Cl}_4]\cdot\text{Et}_4\text{NCl}$.⁴ Each of these clusters contains 12 atoms, with one group 6 metal and three

group 11 metals. Each structure can be viewed as a cube made up of a metal tetrahedron interlocking with a nonmetal tetrahedron, plus a second nonmetal tetrahedron exterior to the cubane and bonded to the metals.

Surprisingly, there have been two different types of statistical distribution invoked in the solution and refinement of the structures. In one the three tetrahedra are presumed to have fixed sites, which may be randomly occupied by each of the atoms constituting the tetrahedron.^{7,8} The cluster is therefore described by just three crystallographic positions. The alternative is to consider the cluster to have a fixed constitution and geometry, which may adopt any of the 12 equivalent orientations permitted by the tetrahedral symmetry about the center.⁹ This orientational disorder could be total, in which nearest neighbors are randomly oriented, or there could be some short-range order that is destroyed by numerous stacking defects.

In this paper we have examined the structure of a homologous group member, $(\text{Bu}_4\text{N})_3[\text{MoCu}_3\text{S}_3\text{OBrI}_3]$, $[\text{MoCu}_3\text{S}_3\text{OBrI}_3]^{3-} = (\mu_3\text{-iodobromodiodotricuprate})\text{oxotri-}\mu_3\text{-thiooxomolybdate}(-3)$, which falls in the space group $F\bar{4}3c$, indicative of a randomized structure. We have attempted to compare both models for statistical distribution of atoms. Other M_4N_8 ($\text{M} = \text{metal}$, $\text{N} = \text{nonmetal}$) clusters have had distinctive nonlinear optical (NLO) properties, and corresponding measurements were undertaken for the title cluster.

Experimental Section

Reagents. $(\text{NH}_4)_2\text{MoO}_2\text{S}_2$ was prepared as described in the literature.¹⁰ Other reagents were analytical grade and were used without further purification.

Synthesis of $(n\text{-Bu}_4\text{N})_3[\text{Cu}_3\text{MoBrI}_3\text{OS}_3]$. A well-ground mixture of $(\text{NH}_4)_2\text{MoO}_2\text{S}_2$ (0.23 g, 1 mmol), CuI (0.40 g, 2

[†] Present address: Department of Chemistry, Santa Clara University, Santa Clara, CA 95053.

[⊗] Abstract published in *Advance ACS Abstracts*, August 1, 1996.

(1) Shi, S.; Ji, W.; Tang, S.-H.; Lang, J.-P.; Xin, X.-Q. *J. Am. Chem. Soc.* **1994**, *116*, 3615.

(2) Shi, S.; Hou, H.-W.; Xin, X.-Q. *J. Phys. Chem.* **1995**, *99*, 4050.

(3) Shi, S.; Ji, W.; Xin, X.-Q. *J. Phys. Chem.* **1995**, *99*, 894.

(4) Shi, S.; Ji, W.; Xie, W.; Chong, T.-C.; Zeng, H.-C.; Lang, J.-P.; Xin, X.-Q. *Mater. Chem. Phys.* **1995**, *39*, 298.

(5) Shi, S.; Ji, W.; Lang, J.-P.; Xin, X.-Q. *J. Phys. Chem.* **1994**, *98*, 3570.

(6) Ji, W.; Shi, S.; Du, H.-J.; Ge, P.; Xin, X.-Q. *J. Phys. Chem.* **1995**, *99*, 7297.

(7) Cai, J.-H.; Weng, L.-H.; Kang, B.-S.; Sang, J.-P.; Zhu, H.-Z.; Xin, X.-Q. *Jiegou Huaxue (J. Struct. Chem.)* **1993**, *12*, 22.

(8) Lang, J.-P.; Xin, X.-Q.; Cai, J.-H.; Kang, B.-S. *Chin. J. Chem.* **1993**, *11*, 418.

(9) Jeannin, Y.; Sécheresse, F.; Bernès, S.; Robert, F. *Inorg. Chim. Acta* **1992**, *198–200*, 493.

mmol), and *n*-Bu₄NBr (0.64 g, 2 mmol) was heated at 95 °C for 10 h under a nitrogen atmosphere. Extraction of the product with CH₂Cl₂ (20 mL) and filtration produced a clear, deep red solution. Dropwise addition of (CH₃)₂CHOH (10 mL) to the top of the red solution produced a two-layer system from which dark red, air-stable crystals (0.20 g) were obtained after standing for a week. Anal. Calcd for C₄₈H₁₀₈BrCu₃I₃MoN₃O₃: C, 36.33; H, 6.86; N, 2.65; Mo, 6.05; Cu, 12.01. Found: C, 35.87; H, 6.52; N, 2.61; Mo, 5.98; Cu, 12.35.

Optical Measurements. Crystals were dissolved in acetonitrile, and the solution was placed in a 1-mm quartz cuvette for optical limiting measurements. The nonlinear optical response was measured with linearly polarized 7-ns pulses ($k = 532$ nm) from a Q-switched, frequency-doubled Nd:YAG laser (Spectra Physics). There was no discernible change in the solution spectrum following irradiation. The spatial profiles of the optical pulses were nearly Gaussian and the light was focused onto the sample with a 25-cm focal length focusing mirror. The spot radius of the laser beam waist was measured to be 35 ± 5 μ m (half-width at $1/e^2$ of the maximum). The interval between the laser pulses was chosen to be 5 s for operational convenience. The incident and transmitted pulse energies were measured simultaneously by two laser precision detectors (RjP-735 energy probes) which were linked to a computer by an IEEE interface.

An identical setup was adopted in experiments to measure the *Z*-scan data, except that the sample was moved along the axis of the incident beam (*Z*-direction) with respect to the focal point, rather than positioned directly at the focal point.¹¹ An aperture of 0.5-mm radius was placed in front of the detector to enable the measurement of the self-defocusing effect.

X-ray Diffraction Data Collection and Reduction. A red crystal approximately 0.3 mm on a side was mounted in a capillary on a Siemens R3m/V X-ray diffractometer. Mo K α radiation (0.710 73 Å) was used. After centering 25 reflections the space group was determined to be $F\bar{4}3c$ (No. 219), with $a = 24.422$ Å. Intensity data were gathered by use of the ω - 2θ scan technique to a maximum 2θ of 45.0°. The structure was solved by direct methods and optimized by full-matrix least-squares, minimizing the weighted function $\sum\{F_o - F_c\}^2/\sigma^2(F)$. Calculations were performed with the SHELXTL PLUS package¹² on a personal computer. The best values of *R* and *R*_w obtained were 0.063 and 0.071, respectively, for the model with a fixed molecular structure and orientation averaging. All non-hydrogen atoms were refined anisotropically, while hydrogen atom positions were calculated and not refined. The crystallographic parameters are summarized in Table 1.

Results and Discussion

Structure. Direct methods indicated that much of the electron density was clustered in three general locations, relative to the origin, plus their tetrahedral symmetry equivalents. Two of the positions generated a cubane structure with the origin at the center. The third position described a tetrahedron outside the cubane, within bonding distance of one of the cubane tetrahedra. Labeling the three positions by the four atoms they comprise, listing the external tetrahedron last and the position to which it is connected first, we suspected the constitution to be {(Cu₃Mo), (S₃Br), (I₃O)}. Isotropic refinement was carried out on the three positions with this distribution of atoms, corresponding to the model with fixed sites and random occupancy. At this point the position of the tetrabutylammonium group could be deduced from the difference Fourier map.

Table 1. Crystallographic Information

empirical formula	C ₄₈ H ₁₀₈ BrCu ₃ I ₃ MoN ₃ O ₃
formula weight	1586.7
color and habit	red prisms
crystal size, mm	0.2 × 0.2 × 0.3
crystal system	cubic
<i>T</i> , K	295
space group	$F\bar{4}3c$ (No. 219)
<i>a</i> , Å	24.422(3)
<i>V</i> , Å ³	14567(7)
<i>Z</i>	8
ρ_{calc} , Mg/m ³	1.447
μ (Mo K α), mm ⁻¹	2.968
scan speed	variable; 2.0 to 29.3°/min in ω
$2\theta_{\text{max}}$	45
reflns collected	1673
independent reflns	395 ($R_{\text{int}} = 6.06\%$)
observed reflns	264 ($F > 4\sigma(F)$)
no. of parameters refined	60
quantity minimized	$\sum w(F_o - F_c)^2$
weighting scheme	$w^{-1} = \sigma^2(F)$
<i>R</i>	0.0633
<i>R</i> _w	0.0708

The difference Fourier also suggested that the external tetrahedron was too heavy and the nonmetal cubane tetrahedron too light. Refinements in which certain atoms and pairs of atoms were given variable occupancy led to the same conclusion. Several variations on the original constitution were tried. Only one, {(Cu₃Mo), (S₃I), (I₂OBr)}, yielded a substantially improved *R* value (0.095 vs 0.125 for the original constitution).

To test orientation averaging of a fixed molecule, each type of atom was assumed to take its own position relative to the origin, for example, all three copper atoms occupied the same position and its tetrahedral equivalents, but the molybdenum was not constrained to share its position with copper. Isotropic refinement led to *R* values of 0.092 for {(Cu₃Mo), (S₃I), (I₂OBr)} and 0.122 for {(Cu₃Mo), (S₃Br), (I₃O)}. The latter model was then discarded. For the former constitution there was still little basis for choosing between site averaging (*R* = 0.095) and orientation averaging (*R* = 0.092). However, with site averaging anisotropic refinement lowered the *R* value only to 0.092, while with orientation averaging it dropped to 0.082. Removal of three reflections for which the difference between the calculated and the observed intensities was greater than 4 σ brought the *R* value to 0.063 using orientation averaging. We conclude that the molecular structure is fixed, with the constitution {(Cu₃Mo), (S₃I), (I₂OBr)}, and this molecule is oriented randomly among the tetrahedrally allowable possibilities. Table 2 lists the atomic coordinates and equivalent isotropic thermal parameters. Bond lengths and bond angles are given in Table 3. Figure 1 is a view of the cubane unit, and Figure 2 is a packing diagram showing the spatial relationship between the Bu₄N⁺ cations and the cubane anion.

Each of the cluster atoms sits at a site with *C*₃ symmetry, when all orientations are averaged. Each *C*₃ axis contains one atom from each of the three tetrahedrons, with the two cubane atoms along a body diagonal. The nitrogen atom from the Bu₄N⁺ cation is at a site of *C*_{4h} symmetry, around which the butyl groups are related by *S*₄ operations.

The known cluster with which (Bu₄N)₃[MoCu₃S₃OBrI₃] is most closely related is (Bu₄N)₃[MoAg₃S₃OBrI₃]. Cai et al.,⁷ using the site-averaging model, placed the bromine atom in the cubane nonmetal tetrahedron, with

(10) McDonald, J. W.; Frieson, G. D.; Rosenheim, L. D.; Newton, W. E. *Inorg. Chim. Acta* **1983**, 72, 205.

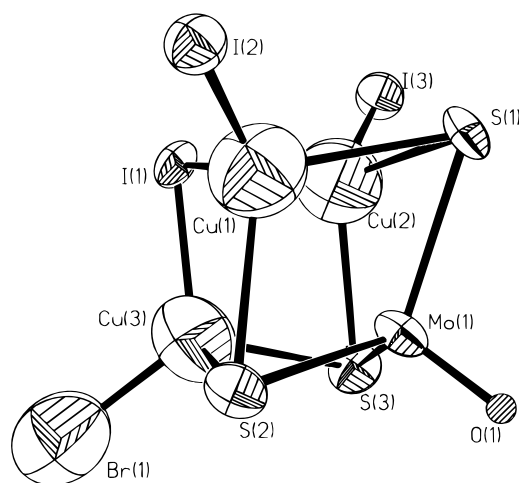
(11) Sheik-Bahac, M.; Said, A. A.; Wei, T.-H.; Hagan, D. J.; Van Stryland, E. W. *IEEE J. Quantum Electron.* **1990**, 26, 760.

(12) Sheldrick, G. M. *SHELXTL PLUS Program for Crystal Structure Solution and Refinement*; Siemens Analytical X-Ray Instruments: Madison, WI, 1990.

Table 2. Atomic Coordinates and Equivalent Isotropic Thermal Parameters ($\text{\AA}^2 \times 10^3$) for $(\text{Bu}_4\text{N})_3[\text{Cu}_3\text{MoOS}_3\text{Br}_3\text{I}]$

atom	site	occupancy	x	y	z	U^a
I1	32e	0.500	0.1059(2)	0.1059(2)	0.1059(2)	139(1)
I2	32e	0.250	-0.0553(6)	0.0553(6)	0.0553(6)	111(4)
Br1	32e	0.250	0.1086(19)	0.1086(19)	0.1086(19)	487(49)
S1	32e	0.750	-0.0691(7)	0.0691(7)	0.0691(7)	131(9)
O1	32e	0.250	0.0827(13)	0.0827(13)	0.0827(13)	1597(177)
Cu1	32e	0.750	0.0471(8)	0.0471(8)	0.0471(8)	388(14)
Mo1	32e	0.250	0.0425(6)	0.0425(6)	0.0425(6)	105(3)
N1	24d	1.000	0	0	0.2500	194(21)
C1	96h	1.000	-0.0470(10)	0.0169(22)	0.2144(12)	427(59)
C2	96h	1.000	-0.0985(17)	0.0385(23)	0.2400(15)	576(75)
C3	96h	1.000	-0.1839(19)	0.0915(26)	0.2196(24)	2051(145)
C4	96h	1.000	-0.1369(16)	0.0593(17)	0.1968(14)	555(65)

^a Equivalent U_{iso} defined as one-third of the trace of the orthogonalized U_{ij} tensor.

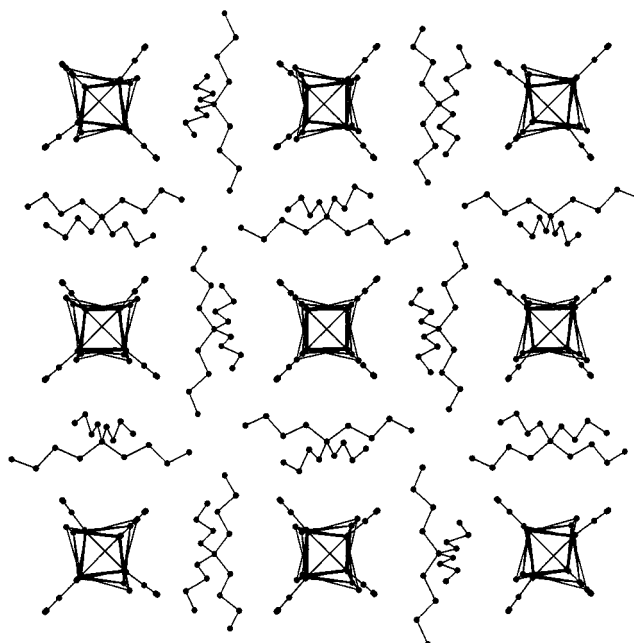
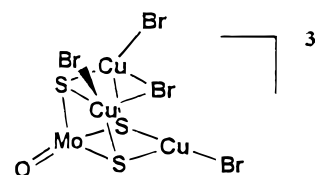
**Figure 1.** ORTEP diagram and atom labeling scheme for the $[\text{Cu}_3\text{MoOS}_3\text{BrI}_3]^{3-}$ cluster.**Table 3. Distances and Angles within the Cluster (\AA ; Refer to Figure 1 for Atom Labels)**

Mo1-S1	2.877(17)	Mo1-O1	1.700(62)
Cu1-S1	2.939(20)	Mo1-Cu1	3.097(36)
Cu1-I1	2.518(23)	Cu1-I2	2.484(37)
Cu3-Br1	2.602(86)		
S1-Mo1-S2	112.2(5)	I1-Cu1-I2	118.8(9)
S1-Mo1-O1	106.6(5)	S1-Cu1-I2	110.3(7)
Mo1-S1-Cu1	64.3(7)	S2-Cu3-S3	108.6(7)
Cu1-S1-Cu2	67.3(10)	S2-Cu3-Br1	110.3(7)
S1-Cu1-S2	108.6(7)	I1-Cu3-Br1	118.8(9)
S1-Cu1-I1	104.1(9)	Cu1-I1-Cu2	80.5(12)

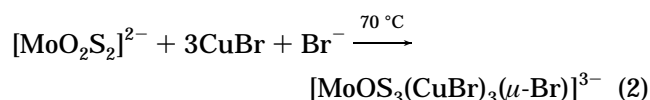
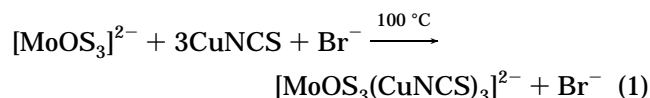
all three iodine atoms in the external nonmetal tetrahedron, in contrast with the present structure in which the bromine is external. Because of orientation averaging, one cannot unambiguously decide which of the atoms in the external tetrahedron (O, Br, or I) is actually bonded to molybdenum, but analogous structures in fixed positions³ strongly suggest it is the oxygen. Likewise, it cannot be unambiguously decided which of the atoms in the cubane nonmetal tetrahedron (I or S) is on the body diagonal with molybdenum. Again, analogous fixed structures suggest it is the iodine.

Relationship of Synthesis to Structure. It has been noted that if molybdenum is introduced into a cluster in the form MoOS_3 , which can be done using either $[\text{MoOS}_3]^{2-}$ or $[\text{MoO}_2\text{S}_2]^{2-}$ as starting material, the resulting cluster tends to have either an open structure (nido skeleton) or a partially open structure (a closo skeleton with one bond broken, as in the $\text{MoCu}_3\text{OS}_3\text{Br}_4$ framework below).

In either case, one oxygen atom is attached to the

**Figure 2.** Packing plot showing the relationship between the cluster anion and the Bu_4N^+ cation. Each atom in the cluster is shown in all its symmetry-equivalent (and orientation averaged) positions.

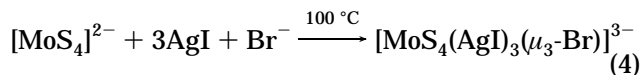
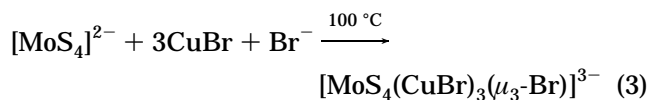
molybdenum through an $\text{Mo}=\text{O}$ double bond.^{4,13-15} On the other hand, a closed cubic cage is readily formed if molybdenum is introduced into a cluster in the form MoS_4 .^{1,7,8} Some representative reactions are



(13) Hou, H.-W.; Xin, X.-Q.; Liu, J.; Chen, H.-Q.; Shi, S. *J. Chem. Soc., Dalton Trans.* **1994**, 3211.

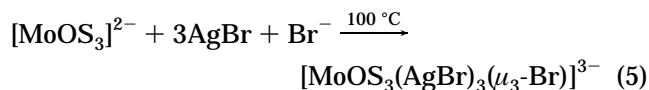
(14) Hou, H.-W.; Ye, X.-R.; Xin, X.-Q.; Liu, J.; Chen, M.-Q.; Shi, S. *Chem. Mater.* **1995**, *7*, 472.

(15) Shi, S.; Chen, Z.-R.; Hou, H.-W.; Xin, Z.-Q.; Yu, K.-B. *Chem. Mater.* **1995**, *7*, 1519.

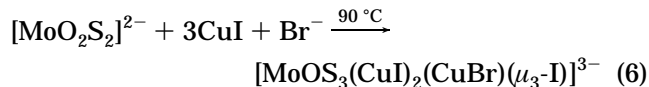


The first cluster above is a nido type (available bromide is not incorporated), while the second is a partially open cubic cage. The third and fourth examples are closed cubic cages. The formation of different final products is probably attributable to subtle differences in the positive charge residing on the copper atoms. In the first two clusters above, the Mo=O group draws electron density toward the terminal oxygen, leaving the copper atoms with a relatively greater positive charge. The more positively charged copper atoms demand in turn more electron density from the bromide. Consequently, the reaction between [MoOS₃(CuBr)₃]²⁻ and Br⁻ is either fruitless (eq 1) or leads only to a partially closed structure (eq 2). In the latter case, after the bromine binds to two copper atoms in the MoOS₃(CuBr)₃ fragment, its binding capability is diminished and coordination to a third copper atom becomes an energetically unfavorable process. This is in contrast to the reaction between [MoS₄(CuBr)₃]²⁻ and Br⁻, in which negative charge from the bromide is equally shared among the three less demanding copper atoms to form the cubane [MoS₄(CuBr)₃Br]³⁻.

When silver replaces copper, there is a similar effect. In [MoOS₃(AgBr)₃(μ₃-Br)]³⁻, the presumably smaller charge on, and greater softness of, the silver atoms, compared to the homologous copper cluster, allows the bromide ion to bind to all three silvers, closing the cage. This cubane-like cluster, unlike the examples above, can be synthesized from the [MoOS₃]²⁻ anion:⁸



The MoCu₃-type cluster of the present study incorporates soft iodine atoms in the cage, which also results in smaller charges on the copper atoms. The resulting cubic cage was synthesized from [MoO₂S₂]²⁻:



Linear and Nonlinear Optical Properties. In addition to clarifying the synthesis/structure issues discussed above, the cluster [MoOS₃(CuI)₂(CuBr)(μ₃-I)]³⁻ was also designed to clarify a relationship between structure and NLO properties.

Previous studies of the NLO properties of Mo-Cu-S(O) clusters have covered a number of structural types, including nest-shaped [MoOS₃Cu₃X₃]²⁻ (X = SCN, Cl, Br, I)^{4,13,14} and cubic cage-shaped [MoS₄Cu₃X'₃Br]³⁻ (X' = Br, I).^{1,5,16} The former exhibit moderate NLO absorption and large NLO refraction (self-defocusing), whereas the latter exhibit strong NLO absorption and very small NLO refraction (self-focusing).

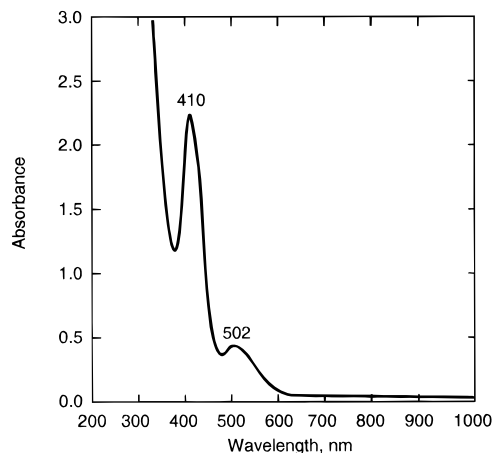


Figure 3. Electronic spectrum of [Cu₃MoOS₃BrI₃]³⁻ in acetonitrile.

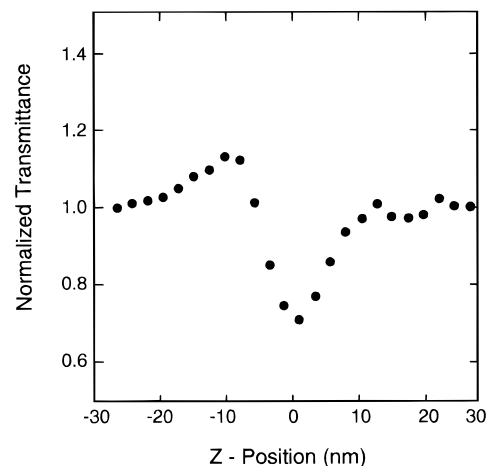


Figure 4. Z-scan data showing both NLO absorption and NLO refraction of the [Cu₃MoOS₃BrI₃]³⁻ cluster.

The question arises, is it the Mo=chalcogenide group (Mo=O or Mo=S) that determines the NLO performance of a cluster, or is it the overall skeletal structure? Previous results were insufficient to answer this question definitively, because each of the nest-shaped clusters studied also had an Mo=O group, and each cubic cage-shaped cluster an Mo=S. The successful synthesis of [MoOS₃(CuI)₂(CuBr)(μ₃-I)]³⁻ provides us a unique opportunity to address this question, since this cluster has both an Mo=O group and a (close) cubic cage-shaped skeletal structure (it should be pointed out that attempts to synthesize a nest-shaped cluster with an Mo=S group have been unsuccessful).

The electronic spectrum of [MoOS₃(CuI)₂(CuBr)(μ₃-I)]³⁻ is shown in Figure 3. Absorption peaks were observed at the following wavelengths (extinction coefficients): 502 nm ($7.3 \times 10^2 \text{ M}^{-1} \text{ cm}^{-1}$) and 410 nm ($3.8 \times 10^3 \text{ M}^{-1} \text{ cm}^{-1}$).

The Z-scan data indicate that the [MoOS₃(CuI)₂(CuBr)(μ₃-I)]³⁻ cluster exhibits both a sizable NLO absorption, as demonstrated by the deep dip near Z = 0 (focal point) in Figure 4, and a sizable NLO refraction, which is self-defocusing, as demonstrated by the peak followed by valley pattern. The behavior of the cluster is thus intermediate between the nest-shaped clusters with an Mo=O group and the cubic cage clusters with an Mo=S. It therefore appears that both the metal-chalcogenide bond and the overall skeletal structure

(16) Du, H.-J.; Ji, W.; Tang, S.-H.; Shi, S. *J. Opt. Soc. Am. B* **1995**, *12*, 876.

influence the NLO properties. In particular, a self-defocusing NLO refraction appears to be associated with the presence of the Mo=O group in the examples studied thus far.

The half-open cage-shaped clusters $[\text{MoS}_3(\text{CuBr})_3(\mu_2\text{-Br})]^{3-}$ ($M = \text{Mo}, \text{W}$) also exhibit NLO behavior intermediate between the cubanes $[\text{MoS}_4(\text{M}'\text{X})_3\text{Br}]^{3-}$ ($M' = \text{Cu}, \text{Ag}; \text{X} = \text{Cl}, \text{Br}, \text{I}$) and the nest-shaped clusters $[\text{MoOS}_3(\text{CuX})_3]^{2-}$ ($\text{X} = \text{Cl}, \text{Br}, \text{I}, \text{NCS}$). When Mo is replaced by W in a half-open cage-shaped cluster, the NLO refraction changes from self-defocusing to self-focusing.¹⁷ The W=O group may be presumed to have an influence similar to that of Mo=S.

NLO properties result from the photodynamic details involving population changes among the ground and excited states.¹⁶ A previous MO analysis shows that the HOMOs of both cubic cage and nest-shaped clusters are mainly Cu-S and Cu-($\mu_3\text{-X}$) bonding in character, while the LUMOs are mainly Mo=S or Mo=O antibonding.¹⁸ It is the structural details of the cluster skeletons that determine the properties of the ground state of the cluster. The Mo=S or Mo=O group exerts its influence mainly on the properties of the lowest excited state.

The NLO absorption of the Mo-Cu-S(O) clusters studied is derived from excited-state absorption¹⁸ from the "LUMO" to higher orbitals. Z-scan data show that the cross section of an electronic transition from the LUMO to a higher orbital is significantly larger than that of the ground-state absorption from the HOMO to the LUMO. In fact, this is true for all members of the families $[\text{MoOS}_3(\text{CuX})_3]^{2-}$ and $[\text{MoS}_4(\text{CuX})_3\text{X}]^{3-}$ as well.

The NLO refractive properties of these clusters are probably controlled by the relative diffuseness of the LUMO compared to the HOMO. Absorption of laser light pumps electrons from HOMO to LUMO, resulting in a transient change in diffuseness (or the extent of delocalization) of the electrons in the outermost shell, and hence the strength of interaction between propagating light and the material (cluster). This change in interaction strength in turn manifests itself as a light-

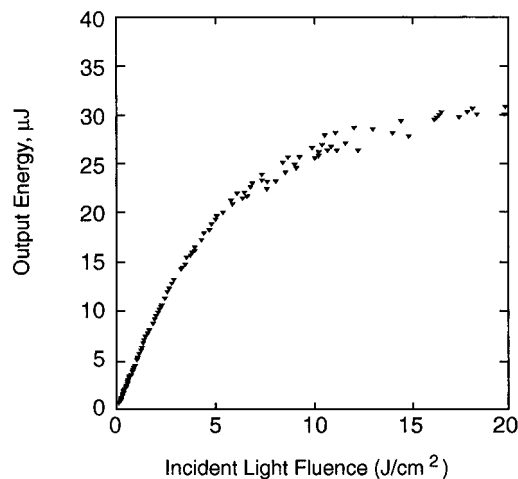


Figure 5. Dependence of the transmitted energy at 532 nm of an acetonitrile solution of $(\text{Bu}_4\text{N})_3[\text{Cu}_3\text{MoOS}_3\text{BrI}_3]$ on the incident light fluence.

induced refractive index change. It is not very surprising that the clusters containing Mo=S exhibit NLO refractive effects different from clusters with an Mo=O group. Electrons should be localized around the Mo=O unit more effectively than around Mo=S. The LUMOs, to which the Mo=O or Mo=S orbitals contribute heavily, will be less diffuse with the Mo=O group, leading to negative refractive index changes.

The optical limiting capability of $[\text{MoOS}_3(\text{CuI})_2(\text{CuBr})(\mu_3\text{-I})]^{3-}$ resulting from the reasonably strong nonlinear absorption at 532 nm is demonstrated in Figure 5. The transmittance begins to deviate from Beer's law when the input light fluence reaches about 1 J/cm^2 , and the material becomes increasingly less transparent as the light fluence rises. The transmitted energy clamps effectively at approximately $30 \mu\text{J}$. The cluster is stable over the dynamic range $0.05\text{--}20 \text{ J/cm}^2$. The transmittance drops from ca. 45% at 1 J/cm^2 to 10% at 20 J/cm^2 .

Supporting Information Available: For $(n\text{-Bu}_4\text{N})_3[\text{Cu}_3\text{MoOS}_3\text{BrI}_3]$, anisotropic thermal parameters and hydrogen atom positions (1 page); structure factor table (1 page). Ordering information is given on any current masthead page.

CM950357F

(17) Chen, Z.-R.; Hou, H.-W.; Xin, X.-Q.; Yu, K.-B.; Shi, S. *J. Phys. Chem.* **1995**, *99*, 8717.

(18) Shi, S.; Lin, Z.-Y.; Mo, Y.; Xin, X.-Q., submitted for publication.